Equal-Gain Combining Receivers over Interference-Limited Nakagami-m Fading with Multiple Cochannel Interferers

Nikos C. Sagias and George S. Tombras
Laboratory of Electronics,
Department of Physics,
University of Athens,
Panepistimiopolis, Zografou, 15236 Athens, Greece
Email: nsagias@space.noa.gr, gtombras@cc.uoa.gr

George K. Karagiannidis
Division of Telecommunications, Electrical and Computer Engineering Department,
Aristotle University of Thessaloniki,
54124 Thessaloniki, Greece
Email: geokarag@auth.gr

Theodoros A. Tsiftsis
Division of Telecommunications, Electrical and Computer Engineering Department,
University of Patras,
Rion, 26500 Patras, Greece
Email: tsiftsis@ee.upatras.gr

***Abstract*— This paper deals with the performance of predetection equal-gain combining (EGC) receivers operating over an interference-limited fading environment with cochannel interference (CCI). It is considered that the desired components of the received signals experience independent, but not necessarily identically distributed, Nakagami-m fading, while the interferers are subjected to independent Rayleigh fading. The analysis is not only limited to identically distributed interferers, but rather includes the case of interferers with distinct average powers. Following the coherent interference power calculation and by using a useful lower-bound for the distribution of the sum of Nakagami-m fading envelopes, novel closed-form upper-bounds for the outage and average symbol error probability for several modulation schemes are presented. Moreover, lower-bounds for the Shannon average spectral efficiency are derived in closed-form. Numerical results demonstrate the effect of the number of the interferers, the number of the receiver branches, and the severity of the fading on the EGC performance. Computer simulations are also performed to verify the tightness and the correctness of the proposed mathematical analysis.**

I. Introduction

Demands for increased capacity cellular networks have forced the systems designers to decrease the channel reuse distances, but according to this design scheme, the overall network capacity can not be made as large as desired. The deliberate reuse of radio channels over relatively short distances limits the reception quality mainly due to cochannel interference (CCI) from adjacent cells [1]. Additionally, the reception quality is further degraded due to the multipath propagation phenomenon and thermal noise. A well-known challenging issue in order to mitigate the impact of fading and CCI is diversity, which is considered as an attractive means for improving the performance of cellular radio networks. Among the most popular diversity techniques, maximal-ratio combining (MRC), equal-gain combining (EGC), and selection combining (SC) are included. EGC presents significant practical interest because it provides better performance than SC and comparable to MRC, but with lower implementation complexity. By comparing the two classical implementations of EGC referred to as predetection and postdetection combining, the former provides better performance than latter at the expense of increased implementation complexity, since channel phase estimation is required. In predetection EGC, the received signals in each of the L antennae are cophased with respect to the desired component, equally weighted, and summed to give the resultant output signal [2].

Several papers have been published in the open technical literature concerning the performance of predetection equal-gain diversity systems under multipath fading (see [2]–[10] and references therein), while a smaller number of works have been presented when CCI is further being considered [11]–[15]. In an early work [11], the outage performance of EGC receivers under Nakagami-m fading channels and CCI has been studied. The same authors, in [12], have analytically derived the average bit error probability (ABEP) of dual-branch EGC receivers with M-ary-phase shift keying (M-PSK) signalling operating over Nakagami-m fading in the presence of Rayleigh CCI. In another related work [13], a useful analytical expression for the outage performance of EGC receivers operating in an interference-limited Rayleigh fading environment with multiple cochannel interferers has been derived, while in [14], the EGC performance for band-limited binary phase shift keying (BPSK) systems operating in Nakagami-m fading with CCI has been analyzed. In that paper, by employing spectrum raised-cosine and Beaulieu-Tan-Damen pulse shapes, the corresponding ABEPs have been analytically derived. Very recently, by following the moments-based approach and the Padé approximants theory, a unified framework for the performance of EGC receivers in the presence of multipath fading, CCI, and additive white Gaussian noise (AWGN) has been presented [15]. In that work, the desired components of the received signals is assumed to experience Rice, Nakagami-m, and Weibull fading, with the interferers being subjected to Nakagami-m fading. However, a unified performance analysis concerning predetection EGC receivers in terms of tabulated functions has not been presented yet. The lack of a such solution stemmes from the difficulty of finding the distribution of the sum of N fading envelopes. In all above mentioned papers, approximative solutions have been given where either a truncation error is involved or the

National Conference on Communications (NCC2006),
New Delhi India, January 2006

results are in the form of unsolved integral with infinite limits. The use of bounds, as opposed to such analytical solutions, serves as a safe method of tackling the performance of EGC receivers in a computational efficient and easy way.

In this paper, the benefits of employing predetection EGC receivers in cellular radio networks are being addressed and studied in terms of tabulated functions. In this effort, independent, but not necessarily identically distributed, Nakagami-m fading and multiple Rayleigh distributed cochannel interferers are being considered. The presented analysis is not limited only to independent and identically distributed (i.i.d.) interferers, but it also includes the important case of independent and not identically distributed (i.n.i.d.) interferers, which more accurately describes realistic cellular wireless channels. Following the coherent interference power calculation and by using a useful lower-bound for the probability density function (PDF) of the sum of Nakagami-m fading envelopes, novel upper-bounds for the outage probability (OP) and average symbol error probability (ASEP) for several modulation schemes as well as lower-bounds for the Shannon average spectral efficiency (ASE) are obtained in closed-form. Computer simulation are also performed in order to verify the tightness of the proposed bounds.

The remainder of this paper is organized as follows. Section II presents the system and channel model, while in Section III, performance bounds for the OP, ASEP, and ASE are obtained in closed-form. Numerical and computer simulations results are presented in Section IV, while concluding remarks are given in Section V.

II. System and Channel Model

Let us consider an N-branch predetection EGC receiver where the desired component of the received signal in each branch undergoes frequency flat fading and AWGN, while it is being corrupted by L independent Rayleigh cochannel interferers. Matched filters with root raised-cosine (RRC) frequency response are being employed at both transmitters and receiver sides. In each branch, the signal is passed through the RRC filter and the sampler, while perfect timing synchronization for the desired user is assumed. After cophasing the received signals in each branch with respect to the phase Φ_ℓ ($\ell = 1, 2, \ldots, N$) of the corresponding desired component and then summed, the complex baseband signal at the output of the EGC receiver can be expressed as

$$S = d_0 \sum_{i=1}^{N} R_i + \sum_{k=1}^{L} \sum_{j=1}^{N} d_k \underbrace{X_{k,j} \exp\left[\jmath\left(\Theta_{k,j} - \Phi_j\right)\right]}_{G_{k,j}} + \sum_{i=1}^{N} C_i \exp\left(-\jmath\,\Phi_i\right) \tag{1}$$

where d_0 and d_ν ($\nu = 1, 2, \ldots, L$) are the desired and νth interfering complex transmitted symbols, respectively, with average energy[1] $E_s = \mathcal{E}\left\langle |d_0|^2 \right\rangle = \mathcal{E}\left\langle |d_\nu|^2 \right\rangle$ ($\mathcal{E}\left\langle\cdot\right\rangle$ denotes expectation), C_ℓ is the AWGN complex sample in the ℓth input branch having single-sided power spectral density N_0 identical to all branches, and $\jmath = \sqrt{-1}$. With R_ℓ, the instantaneous fading envelope of the desired component of the received signal in the ℓth input branch is denoted, with its PDF given by

$$f_{R_\ell}(x) = \left(\frac{m_\ell}{\Omega_\ell}\right)^{m_\ell} \frac{x^{2m_\ell - 1}}{\Gamma\left(m_\ell\right)} \exp\left(-\frac{m_\ell}{\Omega_\ell}\, x^2\right) \tag{2}$$

where $\Omega_\ell = \mathcal{E}\left\langle R_\ell^2 \right\rangle$ and $m_\ell \geq 1/2$ are the average fading power and the Nakagami-m fading parameter, respectively and $\Gamma(\cdot)$ is the Gamma function [16, eq. (8.310/1)]. Moreover in (1), $G_{\nu,\ell} = X_{\nu,\ell} \exp\left[\jmath\left(\Theta_{\nu,\ell} - \Phi_\ell\right)\right]$ is a zero-mean Gaussian complex random variable (RV), expressing the channel gain of the νth interferer in the ℓth input branch multiplied by the cophasing factor $\exp(-\jmath\,\Phi_\ell)$, with $(\Theta_{\nu,\ell} - \Phi_\ell)$ being uniformly distributed in $[0, 2\pi)$ and $X_{\nu,\ell}$ being Rayleigh distributed. We further consider equal average fading power from each interferer to each receiver branch, i.e., $\mathcal{E}\left\langle X_{\nu,\ell}^2 \right\rangle = \overline{P}_\nu$, $\forall \ell$. The usual assumptions are made, that the desired and interfering components are uncorrelated with each other and that the channel is slow fading for both of them.

As in [13], by following the coherent interference power calculation and the Gaussian interference model [17], the instantaneous EGC output SINR per symbol can be expressed as

$$Z = \frac{E_s \left(\sum_{i=1}^{N} R_i\right)^2}{N\,N_0 + a\,E_s \sum_{i=1}^{L} \left|\sum_{k=1}^{N} G_{i,k}\right|^2} = \frac{\frac{E_s}{N_0}\left(\sum_{i=1}^{N} R_i\right)^2}{N + a\,\frac{E_s}{N_0} \sum_{i=1}^{L} I_i} \tag{3}$$

where $a = 1 - \rho/4$ with $0 \leq \rho \leq 1$ being the roll-off factor of both the transmitting and receiving RRC filters and $I_\nu = \left|\sum_{k=1}^{N} G_{\nu,k}\right|^2$ is an exponentially distributed RV with PDF given by

$$f_{I_\nu}(x) = \frac{1}{\overline{I}_\nu} \exp\left(-\frac{x}{\overline{I}_\nu}\right) \tag{4}$$

and $\overline{I}_\nu = N\,\overline{P}_\nu$ being its corresponding average value. The sum of L exponentially distributed RVs appearing in the denominator of (3), can be represented by another RV for the following two cases. In case of equal interferers' powers, i.e., $\overline{P}_\nu = \overline{P}\ \forall \nu$, the PDF of $U = a \sum_{i=1}^{L} I_i$ is given by the Erlang distribution

$$f_U(x) = \frac{1}{(L-1)!\,\left(a\,N\,\overline{P}\right)^L} x^{L-1} \exp\left(-\frac{x}{a\,N\,\overline{P}}\right) \tag{5a}$$

with corresponding average power $\overline{U} = a\,L\,N\,\overline{P}$, while in case of distinct interferers powers, i.e., $\overline{P}_i \neq \overline{P}_j\ \forall i \neq j$, by

$$f_U(x) = \frac{1}{a\,N} \sum_{k=1}^{L} \frac{\Pi_k}{\overline{P}_k} \exp\left(-\frac{x}{a\,N\,\overline{P}_k}\right) \tag{5b}$$

[1] Only constant envelope modulation schemes are being considered to be used with EGC.

with corresponding average power $\overline{U} = a\,N\,\sum_{i=1}^{L}\overline{P}_i$ and

$$\Pi_\nu = \prod_{\substack{i=1\\ i\neq\nu}}^{L} \frac{\overline{P}_\nu}{\overline{P}_\nu - \overline{P}_i}.$$

III. Performance Analysis

Starting with (3), the instantaneous SIR at the output of the EGC can be expressed as

$$\gamma = \frac{1}{\overline{U}}\left(\sum_{i=1}^{N} R_i\right)^2. \tag{6}$$

Using the well-known inequality between the arithmetic and geometric mean [16, Section 11.116] for RVs R_ℓ

$$\frac{1}{N}\sum_{i=1}^{N} R_i \geq \prod_{i=1}^{N} R_i^{1/N} \tag{7}$$

(6) can be lower bounded as

$$\gamma \geq N^2\,\frac{\mathcal{P}^{2/N}}{U} \tag{8}$$

where RV $\mathcal{P}$ is defined as the product of R_ℓ, i.e., $\mathcal{P} = \prod_{i=1}^{N} R_i$, with PDF given by [18, eq. (4)]

$$f_{\mathcal{P}}(x) = \frac{2}{x\prod_{i=1}^{N}\Gamma(m_i)}\,G_{0,N}^{N,0}\left[x^2\prod_{i=1}^{N}\left(\frac{m_i}{\Omega_i}\right)\Big|_{m_1,\,m_2,\ldots,m_N}^{-}\right] \tag{9}$$

where $G[\cdot]$ is the Meijer's G-function[2] [16, eq. (9.301)]. It can be easily recognized, that for the special case of $N = 1$ and by using [19, eq. (11)], (9) reduces to (2).

Since RVs $\mathcal{P}$ and U are mutually independent, by using (8) and [20, eq. (6.43)], an upper-bound for the PDF of γ can be derived as

$$f_\gamma(x) = \frac{N}{2\,N^N}\int_0^\infty y\,(x\,y)^{N/2}\,f_{\mathcal{P}}\left[\left(\frac{x\,y}{N^2}\right)^{N/2}\right]\,f_U(y)\,dy. \tag{10}$$

Next, the performances of EGC are studied for the two cases of equal and distinct interferers' powers.

A. Equal Average Interferers' Powers

By substituting (5a) and (9) in (10), an integral which is not included in tables of classical reference books such as [16] arises. By expressing the exponential functions as Meijer's G-functions [19, eq. (11)], using [19, eq. (21)], and after some mathematical manipulations, the PDF of γ can be derived as

$$f_\gamma(x) = \frac{N^{L+1/2}\left(\sqrt{2\,\pi}\right)^{1-N}}{(L-1)!\,\prod_{i=1}^{N}\Gamma(m_i)}\,x^{-1} \times G_{N,N}^{N,N}\left[x^N\prod_{i=1}^{N}\left(\frac{a\,m_i}{\mathcal{R}_i}\right)\Big|_{m_1,m_2,\ldots,m_N}^{\Delta(N;1-L)}\right] \tag{11}$$

[2]By applying the transformation given by [16, eq. (9.303)] in (9), $G[\cdot]$ can be expressed in terms of more widely used functions, such as the generalized Hypergeometric [16, eq. (9.14/1)]. Both Meijer's G-function and generalized Hypergeometric function are included as built-in functions in most of the popular mathematical software packages such as Maple and Mathematica.

where $\mathcal{R}_\ell = \Omega_\ell/\overline{P}$ is the average SIR of the ℓth input branch and $\Delta(n;x)$ is defined as $\Delta(n;x) \triangleq x/n,\ (x+1)/n,\ldots,\ (x+n-1)/n$, with x an arbitrary real value and n a positive integer.

1) Outage probability: OP is defined as the probability that the instantaneous SIR falls below a given outage threshold γ_{th}. Starting with

$$P_{out}(\gamma_{th}) = \int_0^{\gamma_{th}} f_\gamma(x)\,dx \tag{12}$$

substituting (11), and by using [19, eq. (26)], the OP can be obtained in closed-form as

$$P_{out}(\gamma_{th}) = \frac{N^{L-1/2}\left(\sqrt{2\,\pi}\right)^{1-N}}{(L-1)!\,\prod_{i=1}^{N}\Gamma(m_i)} \times G_{N+1,N+1}^{N,N+1}\left[\gamma_{th}^N\prod_{i=1}^{N}\left(\frac{a\,m_i}{\mathcal{R}_i}\right)\Big|_{m_1,m_2,\ldots,m_N,0}^{\Delta(N;1-L),1}\right]. \tag{13}$$

2) Average symbol error probability: The most straightforward approach to obtain the ASEP, $\overline{P}_{se}$, is to average the conditional symbol error probability $P_{se}(\gamma)$ over the PDF of γ, i.e.,

$$\overline{P}_{se} = \int_0^\infty P_{se}(x)\,f_\gamma(x)\,dx. \tag{14}$$

For $P_{se}(\gamma)$ there are well-known generic expressions for different sets of modulation schemes, including:

i) Binary frequency shift keying (BFSK), BPSK and for higher values of average SIR, differentially encoded BPSK (DEBPSK), quadrature phase shift keying (QPSK), minimum shift keying (MSK), and square M-ary-quadrature amplitude modulation (M-QAM), with $M \geq 4$, in the form of

$$P_{se}(\gamma) = A\,\mathrm{erfc}\left(\sqrt{B\,\gamma}\right) \tag{15}$$

where $\mathrm{erfc}(\cdot)$ is the well-known complementary error function [16, eq. (8.250/4)];

ii) Non-coherent BFSK (NBFSK) and binary differential phase shift keying (BDPSK), in the form of

$$P_{se}(\gamma) = A\,\exp(-B\,\gamma); \tag{16}$$

iii) $\pi/4$-differential QPSK ($\pi/4$-DQPSK) with Gray encoding, M-PSK, and M-ary-differential phase shift keying (M-DPSK), with $M \geq 4$, in the form of

$$P_{se}(\gamma) = A\int_0^\Lambda \exp[-B(\theta)\,\gamma]\,d\theta. \tag{17}$$

In the above expressions for $P_{se}(\gamma)$, the particular values of A, B, and Λ depend on the specific modulation scheme employed and can be found in [21]. Next, (14) is solved in closed-form for each one of the above sets of signals.

Using (11), (14), and (15), it can be easily recognized that for the first set of modulated schemes (i.e., BPSK, BFSK, DEBPSK, QPSK, MSK, and square M-QAM), the evaluation of definite integrals, which include Meijer's, power, and exponential functions, is required. Since this kind of integrals are not tabulated, the solution can be found with the aid of [19,

eq. (21)], so that the ASEP can be expressed in a closed-form as

$$\overline{P}_{se} = \frac{A\,N^{L-1/2}\,(2\,\pi)^{1-N}}{\sqrt{\pi}\,(L-1)!\,\prod_{i=1}^{N}\Gamma\,(m_i)} \times G_{3N,2N}^{\,N,3N}\left[\prod_{i=1}^{N}\left(\frac{a\,N\,m_i}{B\,\mathcal{R}_i}\right)\Big|_{m_1,m_2,\ldots,m_N,\Delta(N;0)}^{\Delta(N;1-L),\Delta(N;1),\Delta(N;1/2)}\right]. \tag{18}$$

Similarly, by substituting (11) and (16) in (14) and by using [19, eq. (21)], for the second set (i.e., NBFSK and BDPSK) the ASEP for can be derived as

$$\overline{P}_{se} = \frac{A\,N^{L}\,(2\,\pi)^{1-N}}{(L-1)!\,\prod_{i=1}^{N}\Gamma\,(m_i)} \times G_{2N,N}^{\,N,2N}\left[\prod_{i=1}^{N}\left(\frac{a\,N\,m_i}{B\,\mathcal{R}_i}\right)\Big|_{m_1,m_2,\ldots,m_N}^{\Delta(N;1-L),\Delta(N;1)}\right] \tag{19}$$

while for the third set (i.e., $\pi/4$-DQPSK with Gray encoding, M-PSK, and M-DPSK), as

$$\overline{P}_{se} = \frac{A\,N^{L}\,(2\,\pi)^{1-N}}{(L-1)!\,\prod_{i=1}^{N}\Gamma\,(m_i)} \times \int_0^{\Lambda} G_{2N,N}^{\,N,2N}\left[\prod_{i=1}^{N}\left(\frac{a\,N\,m_i}{B(\theta)\,\mathcal{R}_i}\right)\Big|_{m_1,m_2,\ldots,m_N}^{\Delta(N;1-L),\Delta(N;1)}\right] d\theta. \tag{20}$$

The integral in the last equation can be evaluated via numerical integration using any of the well-known mathematical software packages (e.g. Mathematica and Maple).

3) Average spectral efficiency: The Shannon capacity of a channel defines its theoretical upper-bound for the maximum data transmission rate at an arbitrarily small bit error rate, without any delay or complexity constraints. Therefore, the Shannon capacity represents an optimistic bound for practical communication schemes, and also serves as a benchmark against which to compare the spectral efficiency of all practical adaptive transmission schemes [22]. In an interference-limited environment without fading the Shannon spectral efficiency is given by $S_e(\gamma) = \log_2(1+\gamma)$. As this equation reads, since $S_e(\gamma)$ is directly connected to γ, it can be also considered as another RV. Hence, the ASE can be obtained by averaging $S_e(\gamma)$ over the PDF of γ [23], i.e.,

$$\overline{S}_e = \int_0^{\infty} \log_2(1+x)\,f_{\gamma}(x)\,dx. \tag{21}$$

By transforming the logarithm to Meijer's G-functions [19, eq. (11)], averaging over the PDF of γ as represented by (11) and (21), and by using [19, eq. (21)], the ASE yields in closed-form as

$$\overline{S}_e = \frac{N^{L-1/2}\,\left(\sqrt{2\,\pi}\right)^{3(1-N)}}{\ln(2)\,(L-1)!\,\prod_{i=1}^{N}\Gamma\,(m_i)} \times G_{3N,3N}^{\,3N,2N}\left[\prod_{i=1}^{N}\left(\frac{a\,m_i}{\mathcal{R}_i}\right)\Big|_{m_1,m_2,\ldots,m_N,\Delta(N;0),\Delta(N;0)}^{\Delta(N;1-L),\Delta(N;0),\Delta(N;1)}\right]. \tag{22}$$

By using (13), the outage spectral efficiency can be also derived in a simple closed-form expression as $P_{ase}(x) = P_{out}\,(2^x - 1)$.

B. Distinct Average Interferers' Powers

By substituting (5b) and (9) in (10) and by using [19, eq. (21)], the PDF of γ can be derived as

$$f_{\gamma}(x) = \frac{N^{3/2}\,\left(\sqrt{2\,\pi}\right)^{1-N}}{\prod_{i=1}^{N}\Gamma\,(m_i)}\,x^{-1}\sum_{k=1}^{L}\Pi_k \times G_{N,N}^{\,N,N}\left[x^{N}\prod_{i=1}^{N}\left(\frac{a\,m_i}{\mathcal{R}_{i,k}}\right)\Big|_{m_1,m_2,\ldots,m_N}^{\Delta(N;0)}\right] \tag{23}$$

where $\mathcal{R}_{\ell,\nu} = \Omega_{\ell}/\overline{P}_{\nu}$ is the average SIR of the νth interferer in the ℓth input branch.

1) Outage probability: Starting with (12), substituting (23), and by using [19, eq. (26)], the OP can be obtained in closed-form as

$$P_{out}\,(\gamma_{th}) = \frac{\sqrt{N}\,\left(\sqrt{2\,\pi}\right)^{1-N}}{\prod_{i=1}^{N}\Gamma\,(m_i)}\sum_{k=1}^{L}\Pi_k \times G_{N+1,N+1}^{\,N,\,N+1}\left[\gamma_{th}^{N}\prod_{i=1}^{N}\left(\frac{a\,m_i}{\mathcal{R}_{i,k}}\right)\Big|_{m_1,m_2,\ldots,m_N,0}^{\Delta(N;0),1}\right]. \tag{24}$$

2) Average symbol error probability: By substituting, (15), and (23) in (14) and by using [19, eq. (21)], for BPSK, BFSK, DEBPSK, QPSK, MSK, and square M-QAM, the ASEP can be expressed in a closed-form as

$$\overline{P}_{se} = \frac{A\,\sqrt{N}\,(2\,\pi)^{1-N}}{\sqrt{\pi}\,\prod_{i=1}^{N}\Gamma\,(m_i)}\sum_{k=1}^{L}\Pi_k \times G_{3N,2N}^{\,N,3N}\left[\prod_{i=1}^{N}\left(\frac{a\,N\,m_i}{B\,\mathcal{R}_{i,k}}\right)\Big|_{m_1,m_2,\ldots,m_N,\Delta(N;0)}^{\Delta(N;0),\Delta(N;1),\Delta(N;1/2)}\right]. \tag{25}$$

Similarly by using (16), for NBFSK and BDPSK, the ASEP for can be also derived as

$$\overline{P}_{se} = \frac{A\,N\,(2\,\pi)^{1-N}}{\prod_{i=1}^{N}\Gamma\,(m_i)}\sum_{k=1}^{L}\Pi_k \times G_{2N,N}^{\,N,2N}\left[\prod_{i=1}^{N}\left(\frac{a\,N\,m_i}{B\,\mathcal{R}_{i,k}}\right)\Big|_{m_1,m_2,\ldots,m_N}^{\Delta(N;0),\Delta(N;1)}\right] \tag{26}$$

while for $\pi/4$-DQPSK with Gray encoding, M-PSK, and M-DPSK, as

$$\overline{P}_{se} = \frac{A\,N\,(2\,\pi)^{1-N}}{\prod_{i=1}^{N}\Gamma\,(m_i)}\sum_{k=1}^{L}\Pi_k \int_0^{\Lambda} \times G_{2N,N}^{\,N,2N}\left[\prod_{i=1}^{N}\left(\frac{a\,N\,m_i}{B(\theta)\,\mathcal{R}_{i,k}}\right)\Big|_{m_1,m_2,\ldots,m_N}^{\Delta(N;0),\Delta(N;1)}\right] d\theta. \tag{27}$$

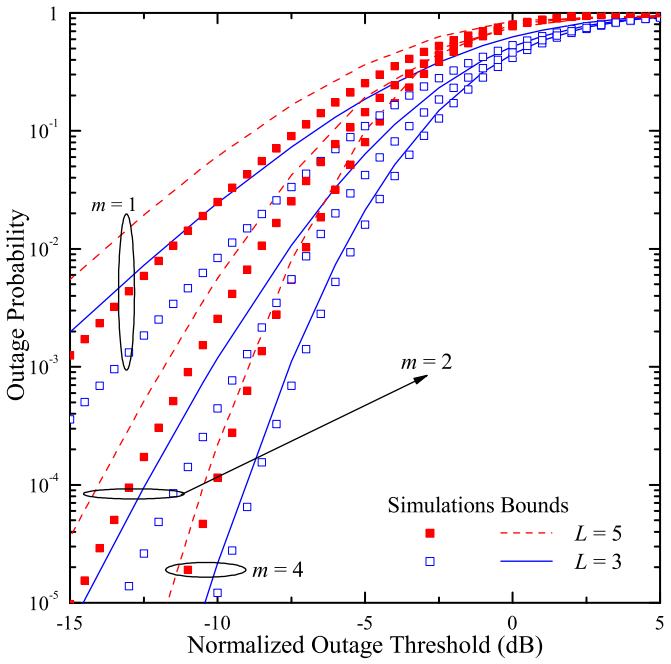

Fig. 1. OP as a function of the normalized outage threshold at the output of EGC receiver with three branches.

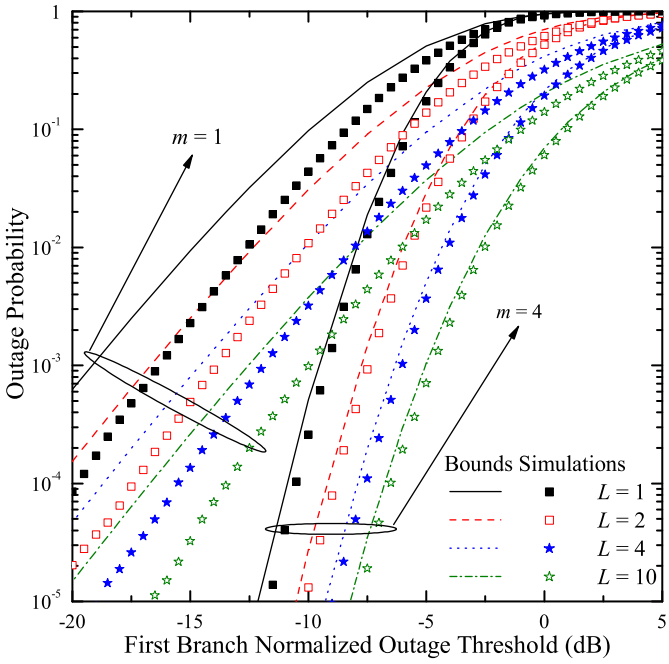

Fig. 2. OP as a function of the normalized outage threshold for i.n.i.d. desired and interfering components at the output of EGC receiver with three branches.

3) Average spectral efficiency: By substituting (23) in (21) and following a similar procedure for the derivation of (22), the ASE for i.n.i.d. interferers can be obtained in closed-form as

$$\overline{S}_e = \frac{\sqrt{N}\left(\sqrt{2\pi}\right)^{3(1-N)}}{\ln(2)\prod_{i=1}^{N}\Gamma(m_i)}\sum_{k=1}^{L}\Pi_k \times G_{3N,3N}^{3N,2N}\left[\prod_{i=1}^{N}\left(\frac{a\,m_i}{\mathcal{R}_{i,k}}\right)\Big|_{m_1,m_2,\ldots,m_N,\Delta(N;0),\Delta(N;0)}^{\Delta(N;0),\Delta(N;0),\Delta(N;1)}\right] \quad (28)$$

while by using (24), the outage ASE can be also derived in a simple closed-form.

IV. Numerical and Computer Simulation Results

In this section, representative performance evaluation results for N-branch EGC receivers operating in the presence of multipath fading and CCI, such as the OP and ABEP for digital communication systems are presented. Without loss of generality, the presented results are for identical values ($m_\ell = m$) and integer-order fading parameters. When i.n.i.d. desired components and/or interferers are being considered, exponentially power delay profiles (PDP)s which are determined by $\Omega_\ell = \Omega_1 \exp\left[-\delta_D\left(\ell-1\right)\right]$ and/or $\overline{P}_\nu = \overline{P}_1 \exp\left[-\delta_I\left(\nu-1\right)\right]$ are being assumed, respectively, with δ_D and δ_I being the respective power decaying factors.

Having numerically evaluated (13) and (24), the performance upper-bounds for the OP, P_{out}, of a three-branch ($N = 3$) EGC receiver are presented, in Figs. 1 and 2, respectively, as a function of the normalized to $\mathcal{R}_1$ outage threshold, $\gamma_{th}/\mathcal{R}_1$, with an exponentially decaying PDP for the desired components of the received signals with $\delta_D = 0.2$ and for several values of m and L. Fig. 1 is plotted for i.i.d. interferers, while in Fig. 2, i.n.i.d. interferers with $\delta_I = 0.2$ are being considered. As expected, the results clearly show that P_{out} improves with a decrease of L and/or $\gamma_{th}/\mathcal{R}_{1,1}$ and/or an increase of m. For comparison purposes, the curves for the corresponding exact P_{out}, obtained via computer simulations, are also included in these figures. By comparing the numerically evaluated results with the computer simulated ones, we deduce a close match between them. Specifically, as m increases, the bounds become tighter. For example, from Fig. 2 for $L = 1$, and $P_{out}(\cdot) = 6 \times 10^{-4}$, for $m = 1$ and $m = 4$, the differences between exacts and bounds are 3 dB and less than 0.3 dB, respectively. The trend of the results can be explained as follows. As it is clear, the lower the difference between the terms of the left hand side (LHS) and right hand side (RHS) of (7), the tighter are the bounds. In fact, equality in (7) holds if and only if all R_ℓ's are equal with each other, i.e., $R_1 = R_2 = \cdots = R_N$. For relatively large values of m, all fading envelopes R_ℓ will be with high probability close to their average value, and thus, it is expected that R_ℓ's will take similar values.

Using (18)–(20) for i.i.d. and (25)–(27) for i.n.i.d. interferers, the ASEP performance upper-bounds of an N-branch EGC receivers, operating in the presence of Nakagami-m fading and CCI, can be numerically evaluated for various coherent or non-coherent and binary or multilevel modulation schemes. As an indicative example, the ABEP performance, $\overline{P}_{be} = \overline{P}_{se}/\log_2(M)$, of Gray encoded 8-PSK ($M = 3$) is illustrated in Fig. 3. In Fig. 3, $\overline{P}_{be}$ is plotted as a function

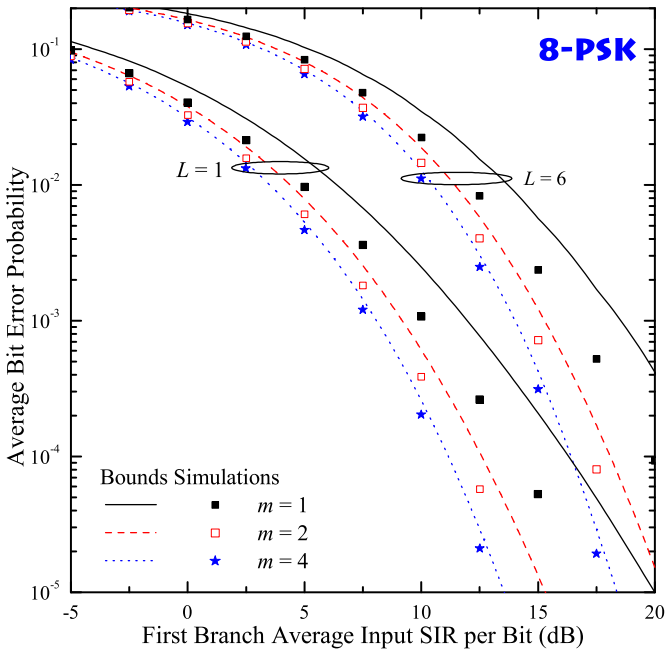

Fig. 3. ABEP performance of 8-PSK signalling for an EGC receiver with four branches operating in a i.n.i.d. Rayleigh fading environment.

of the average SIR per bit of the first input branch, $\overline{\gamma}_b = \mathcal{R}_{1,1}/\log_2(M)$, for a Rayleigh fading environment with 8-PSK signalling, $N = 4$, $\rho = 0.8$, and for several values of L and m. As expected, the obtained performance evaluation results show that $\overline{P}_{be}$ improves with an increase of N and/or m. For comparison purposes, results obtained by means of computer simulations are also included in Fig. 3, verifying the tightness of the proposed bounds. Similarly to Figs. 1 and 2, the numerically evaluated results for the bounded ABEPs are close to the simulated ones, while as previously mentioned the higher m, the tighter the bounds are.

V. Conclusions

The performance of equal-gain diversity receivers operating in an interference-limited environment was studied. Considering independent, but not necessarily identically distributed, Nakagami-m desired and Rayleigh interference components, novel closed-form upper-bounds for the OP and ASEP, and lower-bounds for the ASE were derived in closed-form. Computer simulations were also performed to verify the tightness and the correctness of the proposed mathematical formulation and it was concluded that the higher the value of Nakagami-m fading parameter, the tighter the proposed bounds are.

References

[1] T. S. Rappaport, *Wireless Communications*. USA: Prentice Hall, 1996.

[2] M. K. Simon and M.-S. Alouini, *Digital Communication over Fading Channels*, 2nd ed. New York: Wiley, 2004.

[3] G. K. Karagiannidis, D. A. Zogas, and S. A. Kotsopoulos, "BER performance of dual predetection EGC in correlative Nakagami-m fading," *IEEE Trans. Commun.*, vol. 52, no. 1, pp. 50–53, Jan. 2004.

[4] ——, "Statistical properties of the EGC output SNR over correlated Nakagami-m fading channels," *IEEE Trans. Wireless Commun.*, vol. 3, no. 5, pp. 1764–1769, Sept. 2004.

[5] G. K. Karagiannidis, "Moments-based approach to the performance analysis of equal gain diversity in Nakagami-m fading," *IEEE Trans. Commun.*, vol. 52, no. 5, pp. 685–690, May 2004.

[6] N. C. Beaulieu and A. A. Abu-Dayya, "Analysis of equal gain diversity on Nakagami fading channels," *IEEE Trans. Commun.*, vol. 39, no. 2, pp. 225–234, Feb. 1991.

[7] Q. T. Zhang, "Probability of error for equal-gain combiners over Rayleigh channels: Some closed-form solutions," *IEEE Trans. Commun.*, vol. 45, no. 3, pp. 270–273, Mar. 1997.

[8] ——, "A simple approach to probability of error for equal gain combiners over Rayleigh channels," *IEEE Trans. Veh. Technol.*, vol. 48, no. 4, pp. 1151–1154, July 1999.

[9] C. Iskander and P. T. Mathiopoulos, "Performance of M-QAM with coherent equal-gain combining in correlated Nakagami-m fading," *Electron. Lett.*, vol. 39, no. 1, pp. 141–142, Jan. 2003.

[10] ——, "Analytical level-crossing rates and average fade durations for diversity techniques in Nakagami fading channels," *IEEE Trans. Commun.*, vol. 50, no. 8, pp. 1301–1309, Aug. 2002.

[11] A. A. Abu-Dayya and N. C. Beaulieu, "Outage probabilities of diversity cellular systems with cochannel interference in Nakagami fading," *IEEE Trans. Veh. Technol.*, vol. 41, no. 4, pp. 343–355, Nov. 1992.

[12] ——, "Diversity MPSK receivers in cochannel interference," *IEEE Trans. Veh. Technol.*, vol. 48, no. 6, pp. 1959–1965, Nov. 1999.

[13] Y. Song, S. D. Blostein, and J. Cheng, "Exact outage probability for equal gain combining with cochannel interference in Rayleigh fading," *IEEE Trans. Wireless Commun.*, vol. 2, no. 5, pp. 865–870, Sept. 2003.

[14] K. Sivanesan and N. C. Beaulieu, "Exact BER analysis of bandlimited BPSK with EGC and SC diversity in cochannel interference and Nakagami fading," *IEEE Commun. Lett.*, vol. 8, no. 10, pp. 623–625, Oct. 2004.

[15] D. A. Zogas, N. C. Sagias, and G. K. Karagiannidis, "Equal-gain combining over generalized fading channels with multiple cochannel interferers and AWGN," *IEEE Trans. Veh. Technol.*, vol. 54, 2005.

[16] I. S. Gradshteyn and I. M. Ryzhik, *Table of Integrals, Series, and Products*, 6th ed. New York: Academic, 2000.

[17] A. A. Abu-Dayya and N. C. Beaulieu, "Bandwidth efficient QPSK in cochannel interference and fading," *IEEE Trans. Commun.*, vol. 43, no. 9, pp. 2464–2474, Sept. 1995.

[18] G. K. Karagiannidis, N. C. Sagias, and P. T. Mathiopoulos, "The $N*$ Nakagami distribution: Theory and applications for communications over fading channels," *IEEE Trans. Commun.*, Submitted.

[19] V. S. Adamchik and O. I. Marichev, "The algorithm for calculating integrals of hypergeometric type functions and its realization in REDUCE system," in *Proc. International Conference on Symbolic and Algebraic Computation*, Tokyo, Japan, 1990, pp. 212–224.

[20] A. Papoulis, *Probability, Random Variables, and Stochastic Processes*, 3rd ed. McGraw-Hill, 1991.

[21] S. Sampei, *Applications of Digital Wireless Technologies to Global Wireless Communications*. London, UK: Prentice Hall, 1997.

[22] M. Alouini and A. Goldsmith, "Capacity of Rayleigh fading channels under different adaptive transmission and diversity-combining techniques," *IEEE Trans. Veh. Technol.*, vol. 48, no. 4, pp. 1165–1181, July 1999.

[23] F. Lazarakis, G. S. Tombras, and K. Dangakis, "Average channel capacity in a mobile radio enviroment with Rician statistics," *IEICE Trans. Commun.*, vol. E77-B, no. 7, pp. 971–977, July 1994.